JOURNAL OF MATERIALS SCIENCE 33 (1998) 4621–4626

Characterization of Ge–Bi–S glass by thermal, electrical, switching and optical measurements

K. SEDEEK
Physics Department, Faculty of Science (Girls) AL-Azhar University, Cairo, Egypt
M. FADEL, M. A. AFIFI
Physics Department, Faculty of Education, Ain Shams University, Cairo, Egypt

A study of the synthesized $Ge_{22.5}Bi_7S_{70.5}$ glassy system has been carried out. Differential thermal analysis data indicate the retention in the as-quenched sample of two amorphous phases. Thermal conductivity, ψ, measurements on bulk sample reveal that the main contribution to ψ is due to phonon thermal conductivity. Thermal evaporation of the synthesized ingot gives films with $Ge_{20.7}Bi_{6.8}S_{72.5}$ as composition. The values of the activation energy and the pre-exponential factor calculated from the direct current electrical conductivity above 53 °C suggest that carrier conduction occurred between extended states in these films. The I–V characteristics in the off-state and the switching phenomenon are investigated. A memory switch with a threshold voltage decreasing with temperature is detected for the studied films. Optical parameters such as absorption coefficient, optical gap and refractive index are also determined. Comparison with binary Ge–S glass reveals that the addition of Bi introduces additional absorbing states at band edges.

1. Introduction

Bi–Ge chalcogenide glasses have received great attention [1–5]. In contrary to other Ge chalcogenide glasses, which are normally always p-type, even with the addition of impurities, the ternary alloys $Bi_xGe_{0.2}S_{0.8-x}$, with x in the vicinity of 0.07, can switch the conduction from p- to n-type. Several mechanisms have been given to account for conduction-type reversal. Nagel *et al.* [6] have carried out extensive measurements of material characteristics. They proposed their model of percolating Bi_2B_3 (B = S or Se) regions. Tohge *et al.* [7] assumed that the six-fold co-ordinated Bi atoms in $Bi_xGe_{0.2}B_{0.8-x}$ produce Bi^-, explaining the n-type conductivity.

Elliot and Steel [8] have undertaken EXAFS measurements on a series of samples with $x \geqslant 0.06$: a mechanism involving the suppression of positively charged structural defects and the consequent unpinning of the Fermi level is proposed to account for the doping effect. Bahatia *et al.* [9, 10] studied X-ray diffraction (XRD), differential thermal analysis (DTA) and electrical measurements under high pressure. They argue that carrier type reversal is due to the effect of Bi dopants on the positive correlation energy defect present in Ge chalcogenides. Phillips [11] used the constraint theory to give a two-phase model with $x = 0.06$ as the threshold for the transition.

Recent structural studies of Ge–Bi–S (Se) glasses by Raman spectroscopy and XRD are performed and many results are reported [12–14]. The Raman spectrum reveals a new broad asymmetric peak at 175 cm^{-1} whose intensity increases with Bi content. This is attributed to the Bi_2S_3 structural unit [14].

This paper reports some new results of a systematic study for amorphous Ge–Bi–S chalcogen prepared as bulk or evaporated films. XRD and DTA have been carried out to test the structure. Thermal conductivity, direct current (d.c.) conductivity and switching phenomenon have been studied. Characterization of the optical parameters such as optical gap, absorption coefficient and refractive index is also given. Comparison with some results of the binary Ge–S glass prepared under the same conditions has been also considered.

2. Experimental procedure

The bulk glass Ge–Bi–S was prepared in the convential way [15] by melting a mixture of five nine-purity elements in an evacuated silica ampoule (total batch 5 gm) at 1000 °C for 15 h with continuous rotation. The ampoule was then quenched in ice water. Thermal evaporation of the studied films was carried out using an Edwards E-306A coating unit under conditions mentioned elsewhere [5]. The films were deposited onto corning glass substrate for electrical conductivity and optical measurements and onto pyrographite for switching experiments.

Structural investigation was carried out using an XRD equipped with nickel filtered CuK_α radiation (wavelength $\lambda = 0.154$ nm). DTA of the prepared material was performed using a Shimadzu model DT-30 with a uniform heating rate of 10 °C min^{-1}. Chemical analyses of both bulk and thin film material were monitored by carrying out quantitative analysis (energy dispersive spectroscopy, EDX) on a Joel 6400

scanning electron microscope with a Link-eXL EDS detector. The data were processed through a ZAF correction program contained within the Link-eXL package.

Thermal conductivity was measured for bulk samples (0.326 cm) in a home-made cell using the steady state longitudinal heat flow divided bar method [16]. Electrical conductivity and thermoelectric power measurements for films were carried out under vacuum (10^{-3} Pa) in a specially designed cryostat. Gold electrodes of 1 cm long and distant by 0.1 and 1.5 cm, respectively, for conductivity and thermoelectric power measurements were evaporated into the film in a coplanar configuration. For thermoelectric power measurements two heaters immersed in the port-substrate are controlled to give a temperature difference of 2 °C between the two electrodes. The induced potential difference was recorded using 616-Keithley electrometer. The switching experiments were carried out with the sample sandwiched between two brass electrodes. The details of the used cryostat are given elsewhere [17]. The transmittance, T, and the reflectivity, R, patterns for optical measurements were obtained in the spectral range 0.35–2 μm for normal incidence on the film surface using a double beam Perkin Elmer spectrophotometer model Lambda-9. A virgin corning glass substrate was placed in the reference compartment of the apparatus to obtain the exact T and R patterns of the studied film.

3. Results and discussion

3.1. Structure and composition

The EDX analysis give the compositions $Ge_{22.5}Bi_7S_{70.5}$ and $Ge_{20.7}Bi_{6.8}S_{72.5}$ for the as-quenched material and the evaporated thin films, respectively. These results reveal that there is a change in the chemical composition of the starting material during the evaporation process. A content of Bi of approximately 7 at % was chosen as it was detected to give very interesting properties [6–8].

As the synthesized material was only 5 gm weight and quenched in ice water, it is expected that the incorporated Bi content is most favourable for glass formation. The absence of crystallinity is confirmed by the XRD pattern given in Fig. 1. Typical DTA thermograms of the studied glass, in powder form, are illustrated in Fig. 2. Well resolved double crystallization peaks, T_{c_1} and T_{c_2} at 370 and 505 °C, respectively, with two glass transitions, T_{g_1} and T_{g_2}, at 280 and 430 °C are observed. These results reveal the presence of two phases in the $Ge_{22.5}Bi_7S_{70.5}$ glass studied.

3.2. Transport properties

3.2.1. Thermal conductivity

The thermal conductivity, ψ, of a semiconducting material can be defined with respect to a steady state flow of heat along a specimen within which there exists a temperature gradient, ΔT as [16]

$$\psi = \chi(dT/dx)/\Delta T \quad (1)$$

where χ is the thermal conductivity coefficient of the brass rod ($\chi = 0.16\,cal\,cm^{-1}\,s^{-1}\,k^{-1}$ as determined

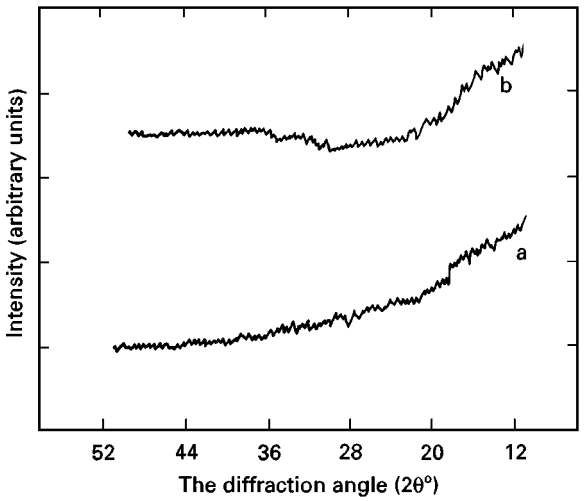

Figure 1 The XRD pattern of as-quenched material (a) and evaporated film (b).

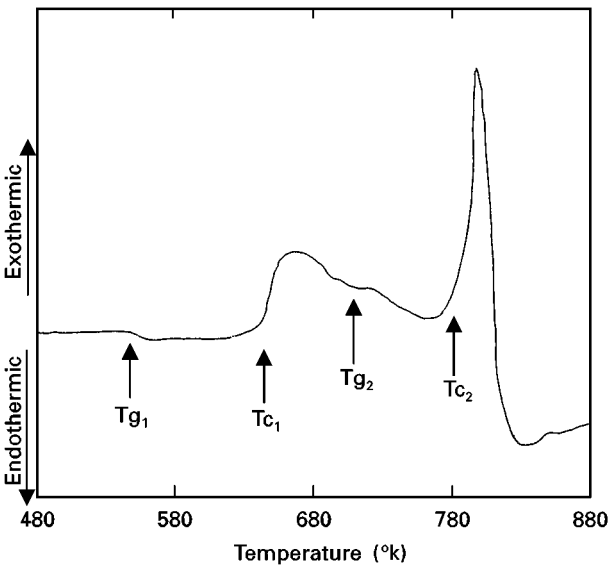

Figure 2 Typical DTA thermogram of the material in powder form.

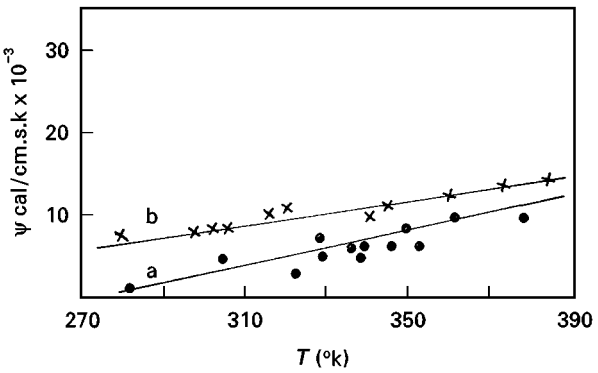

Figure 3 The temperature dependence of the thermal conductivity, ψ, of the bulk sample (a). For comparison, a plot ψ(T) of binary $Ge_{24}S_{76}$ glass is also given (b).

experimentally) and dT/dx is the temperature gradient across it. The thermal conductivity of the $Ge_{22.5}Bi_7S_{70.5}$ glass was measured as a function of temperature up to a value well below the corresponding T_g. The results obtained are plotted in Fig. 3. For

comparison, the results of $Ge_{24}S_{76}$ glass are also given [18]. As observed, the thermal conductivity increases with temperature in the considered range.

It is well known that the thermal energy is transferred through the specimen at $T > 300\,K$ by phonon (lattice vibration), electrons, electron–hole pairs (bipolar) and photons [19]. The contribution of these carriers to ψ are considered to be additive. The electronic and bipolar thermal conductivity, ψ_e and ψ_{bp}, have been calculated for the samples studied using the Wiedman–Franz law [20]

$$\psi_e = L\delta_{25}T \tag{2}$$

$$\psi_{bp} = (3/4\pi^2)\psi_e[(\Delta E/kT) + 4]^2 \tag{3}$$

where L is the Lorenz number, ΔE the conduction activation energy, T the absolute temperature, k the Boltzmann constant and δ the d.c. electrical conductivity.

The values of ψ_e and ψ_{bp} measured at 25 °C are, respectively, 8.69×10^{-14} and 3.29×10^{-11} cal cm^{-1} s^{-1} k^{-1} for $Ge_{24}S_{76}$ and 4.2×10^{-13} and 5.9×10^{-11} cal cm^{-1} s^{-1} k^{-1} for the ternary $Ge_{22.5}Bi_7S_{70.5}$. Although the contribution of ψ_{bp} is greater than ψ_e by about two orders of magnitude, both of them can be neglected as compared with the measured thermal conductivity given in Fig. 3. The photon contribution is also excluded because it is reported to be only effective at high temperature [21]. Thus one can argue that the main contribution to the thermal conductivity of the studied samples is due to phonon thermal conductivity, ψ_{ph}. This can be calculated in solids by the simple Debye expression [22]

$$\psi_{ph} = \tfrac{1}{3} C_v v_{ph} L \tag{4}$$

where C_v is the thermal capacity per unit volume, v_{ph} the propagation velocity and L the main free path of the thermal waves.

L (taken to be in the order of the average distance between ordering regions in amorphous semiconductors, i.e. approximately 1.2 nm) is assumed to control the variation of ψ_{ph} as both C_v and v_{ph} of solids were found to depend weakly on temperature [23, 24]: i.e. the variation of ψ with temperature given in Fig. 3 can be attributed to the trend of L with temperature.

The plots of $\psi(T)$ given in Fig. 3 also show that the addition of Bi to the binary glass decreases the value of ψ all over the studied temperature range. The structure of Ge_xS_{1-x} glass in the S rich region was described by Phillips [25] to be dominated by $(S)_n$ chains and $Ge(S_{1/2})_4$ corner-sharing tetrahedral. As Bi is added, this structure is detected by Raman spectroscopy [14, 26] to be composed of GeS_4 and Bi_2S_3 structural units with S_8 molecules incorporated in the structural network. These structural changes may increase lattice crosslinking, thereby decreasing the phonon mean free path. This may explain the decrease detected for the thermal conductivity of the ternary glass with respect to the binary one as displayed in Fig. 3.

3.2.2. Electrical conductivity

The plot of d.c. electrical conductivity, δ, as a function of temperature for studied $Ge_{20.7}Bi_{6.8}S_{72.5}$ amorphous films with a thickness of 1.852 μm is given in Fig. 4. As shown in the figure, the plot of $\delta(1/T)$ gives a straight line over the temperature region above $T = 53$ °C. It can therefore be described by the Arrhenius relation [27]

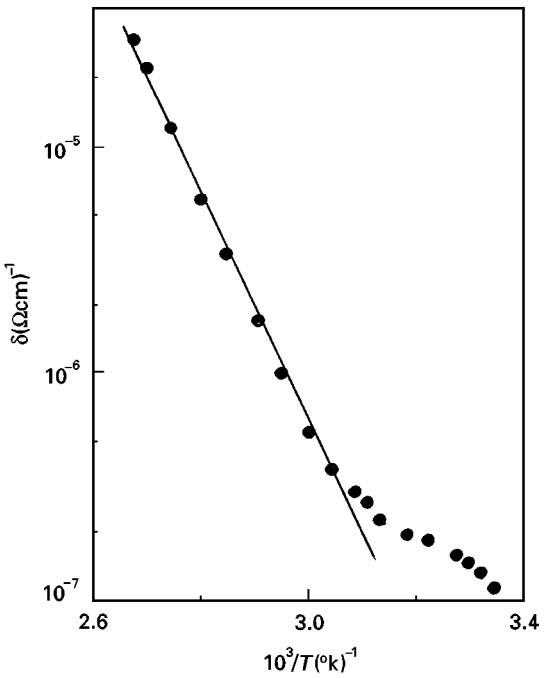

Figure 4 D.c. electrical conductivity, δ, as a function of temperature for the film studied.

$$\delta = C\exp(-\Delta E/kT) \tag{5}$$

where C is the pre-exponential factor. Values of δ_{25} (the conductivity measured at 25 °C, ΔE and C are, respectively, 2.2×10^{-7} $(\Omega\,cm)^{-1}$, 0.99 eV and 3.5×10^{10} $(\Omega\,cm)^{-1}$. These high values of both ΔE and C suggest that electrical conduction takes place between extended states beyond the mobility edges [27]. Below $T = 53$ °C, the plot deviates from linearity, thus reflecting the beginning of a second conduction mechanism due to the onset of hopping conduction between localized states. These states may arise from the lack of long-range order in the amorphous network.

Bhatnager *et al.* [28] give $\Delta E = 0.88$ eV for $Ge_{20}Bi_4S_{76}$ bulk glass, while Tichy *et al.* [29] reported a value of 0.97 eV for $Ge_{28.1}Bi_{6.3}S_{65.6}$. A systematic study of the variation of resistivity with composition for Ge–Bi–S bulk glasses gives evidence that d.c. electrical conductivity in these bulk glasses can be controlled by percolation and, consequently, the transition from p- to n-type conduction appears at a percolation threshold of 7–9 at % Bi [29]. Our studied $Ge_{20.7}Bi_{6.8}S_{72.5}$ films were also detected to exhibit n-type conduction, as a negative sign of the Seeback coefficient is detected for these films.

3.2.3. Switching

Switching consists of the transition from a state of high resistance (OFF) to one of low resistance (ON). The transition is generated by the application of a specific voltage called the threshold voltage, V_{th}. In

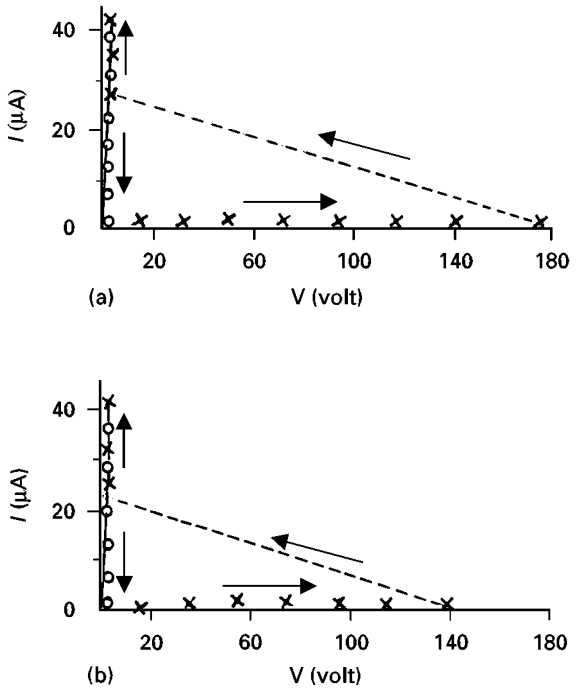

Figure 5 The static I–V characteristic curve of the film studied (a). Results of the amorphous $Ge_{24}S_{76}$ film (b) are also given. Symbols (×) and (o) refer, respectively, to the data taken with increasing and decreasing voltage.

memory switching once the current is suppressed, the ON state remains. The switching phenomenon has been detected for various chalcogenide glasses [30, 31]. In fact, memory switches have been widely used in memory circuits and logic arrays [31].

Both static and dynamic I–V characteristic curves were studied for the $Ge_{20.7}Bi_{6.8}S_{72.5}$ film of 1.852 μm thickness. The room temperature static I–V characteristic of this composition is given in Fig. 5. Results of the binary $Ge_{24}S_{76}$ films are also given for comparison. As shown in the figure, the curves have characteristics typical of a memory switch. In this case the amorphous film underwent structural alteration. This does not mean full ordering to the crystalline state occurred. Rather, under the action of a high electric field the structural units changed position and bonding status. As a result, highly conductive regions (channels) were formed in the amorphous network.

It is assumed that the thermal effect causing the structural alteration rose by Joule heating, caused by leakage of the current prior to switching [31]. Lower values of the threshold voltage are therefore expected to occur as at which the I–V data are detected the temperature of the film is increased. To investigate the variation of threshold voltage with temperature, V_{th} was recorded for each composition at different temperatures ranging between 22 and 100 °C ($< T_g$). The results show a decrease of V_{th} with increasing temperature. The plots of ($\ln V_{th}$) versus ($10^3/T$) for the compositions studied yield straight lines, as illustrated in Fig. 6. The dependence of V_{th} on temperature can therefore be expressed by [32]

$$V_{th} = V_0 \exp(E/kT) \tag{6}$$

where V_0 is a constant and E is the threshold voltage activation energy. The observed temperature

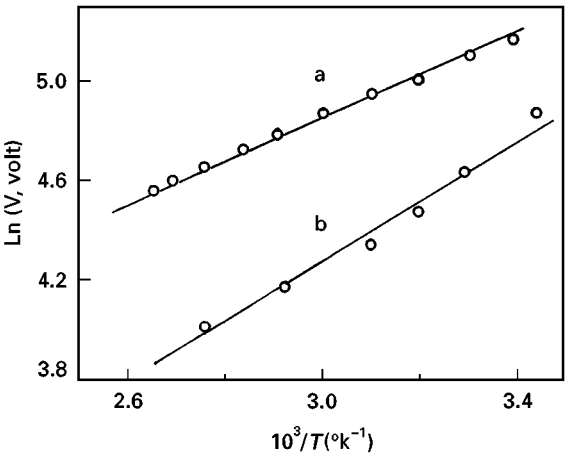

Figure 6 Temperature dependence of the threshold voltage, V_{th}, for the film studied (a) and for binary $Ge_{24}S_{76}$ film (b).

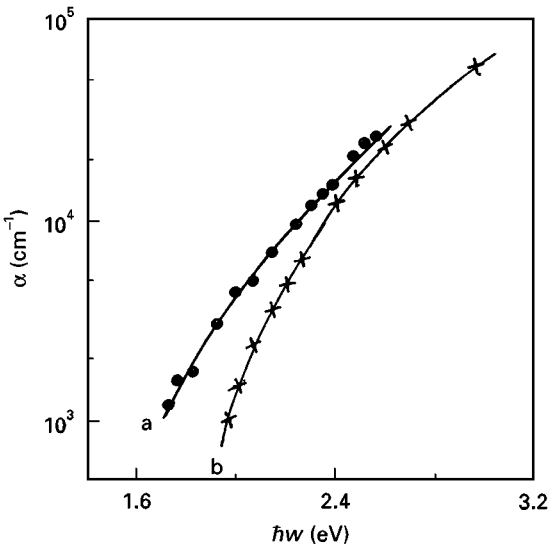

Figure 7 Variation of absorption coefficient, α, with photon energy, $\hbar w$, for the film studied (a). Results for the amorphous $Ge_{24}S_{76}$ film are also given (b).

dependence of the threshold voltage on temperature can be understood in terms of a thermal model for the preswitching region. The switching process itself is interpreted as an electronic process brought about by thermal effects. The trend of the threshold voltage with temperature has a small value of slope, as values of $E = 0.22$ and 0.19 eV were calculated, respectively, for the binary and the ternary films studied. Values of 0.18 and 0.41 eV were determined, respectively, for $Ge_{20}Te_{70}Se_{10}$ and $Se_{70}Ge_{10}Sb_{20}$ glasses [33, 34].

3.3. Optical properties

The absorption coefficient, $\alpha(w)$, is calculated for the $Ge_{20.7}Bi_{6.8}S_{72.5}$ films studied according to the relation [35]

$$\alpha(w) = (1/d)\ln[(1 - R)^2/T] \tag{7}$$

where d is the film thickness. Fig. 7 shows the variation of $\alpha(w)$ with photon energy, $\hbar w$, for the film studied ($d = 1.852$ μm). The plot of $(\alpha\hbar w)^{1/2}$ versus $\hbar w$

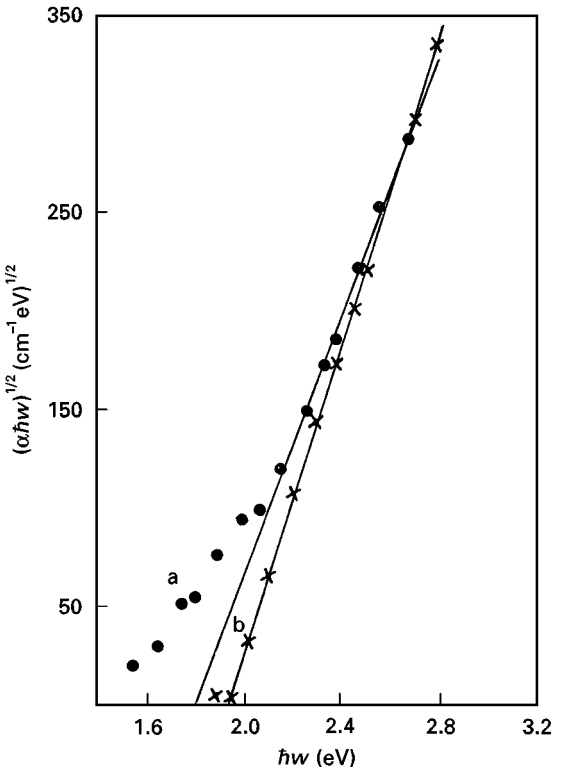

Figure 8 A plot of $(\alpha\hbar w)^{1/2}$ versus $\hbar w$ for the film studied (a) and for the binary $Ge_{24}S_{76}$ film (b).

is given in Fig. 8 for the same sample. Results for the binary $Ge_{24}S_{76}$ film are also plotted for comparison. The intersect of the straight line with the abscissa in Fig. 8 gives the optical gap, E_0, according to the relation [36, 37]

$$\alpha\hbar w = \beta(E_0 - \hbar w)^s \tag{8}$$

where β^{-1} is the edge width parameter, with $s = 2$ and $E_0 = 1.8$ eV for the ternary composition. Tichy *et al.* [29] reported a value of 1.97 eV for E_{0_3} (the optical gap at $\alpha = 10^3\,cm^{-1}$). The additional absorption tail shown at lower energies in Fig. 8 indicates that the presence of Bi creates some defect and/or energy disorder states located at the band edges.

The refractive index, n, can be calculated in the long-wavelength region where the material is weakly absorbing according to the relation

$$4nd = M\lambda \tag{9}$$

where M is an integer (even at the transmittance maxima). The values $1/\lambda$ at the interference maxima in the experimental transmittance spectrum were used to obtain the order M [38, 39]. Fig. 9 gives the variation of n with λ for the $Ge_{20.7}Bi_{6.8}S_{72.5}$ film studied. It is clear that n varies slightly with λ over the energy range studied.

The effect of annealing on the value of n has been also studied. Fig. 9 displays the variation of n with λ measured after annealing the same film at 120 °C for 2 h. As shown in the figure, n increases from 2.38 to 2.74 at low energy ranges ($\hbar w = 0.68$ eV). Since n in the low absorbing region is related to the static dielectric constant, ε_1, expressed by [40]

$$\varepsilon_1 = n^2 = 1 + 2/3(\hbar w_p/E_G)^2 \tag{10}$$

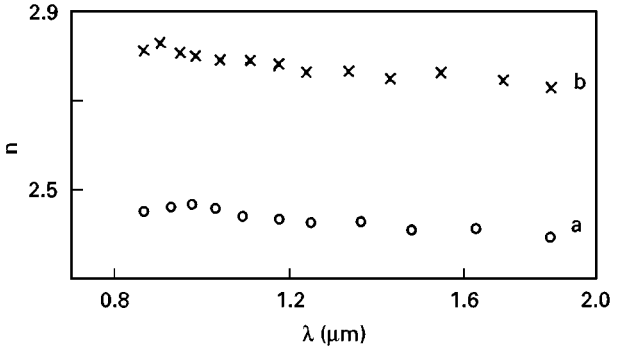

Figure 9 Variation of the refractive index, n, with the wavelength, λ, for the film studied: as deposited (a) and annealed at 120 °C (b).

where w_p is the plasma frequency of the valence electrons, related to the material density; and E_G the Penn gap which determines the bond strength. The increase recorded for n may hence be attributed to the detectable increase in the density of the material from 4.37 to 4.66 gm cm^{-3} with annealing at 120 °C.

4. Conclusions

We have undertaken a systematic study of synthesized $Ge_{22.5}Bi_7S_{70.5}$. DTA reveals the retention of two truly glassy phases in this system. These data clearly indicate that the addition of approximately 7 at % Bi to the Ge–S system modifies the structure of the amorphous network.

The thermal conductivity, ψ, experiments on bulk samples show that the main contribution to ψ is due to lattice thermal conductivity and that ψ increases with increasing temperature. Comparison with the binary $Ge_{24}S_{76}$ glass shows that Bi addition decreases slightly the thermal conductivity due to greater cross-linking of the amorphous network.

Thermal evaporation of the synthesized $Ge_{22.5}Bi_7S_{70.5}$ yields films with an excess of S atoms and a corresponding deficit in those of Ge. The composition of the evaporated films is $Ge_{20.7}Bi_{6.8}S_{72.5}$. The d.c. electrical conductivity measurements of the n-type films give a value of 0.99 eV for thermal activation energy for carriers excited between extended states. The static I–V characteristic curves of the deposited films give evidence for a memory switch with a threshold voltage, V_{th}, decreasing with temperature. Optical investigation of the films gives an optical gap of 1.8 eV and a refractive index, n (0.68), of 2.74. Comparison with the binary $Ge_{24}S_{76}$ system indicates that Bi addition introduces some defects and/or disorder that create additional absorbing states at band edges.

References

1. A. V. PAZIN and Z. U. BORISOVA, *J. Appl. Chem. USSR* **43** (1970) 1225.
2. N. TOHGE, Y. YAMAMOTO, T. MINAMS and M. TANAKA, *J. Appl. Phys. Lett.* **34** (1979) 640.
3. K. L. BAHATIA, *J. Non-Cryst. Solids* **54** (1983) 173.
4. R. MOTHUR and A. KUMAR, *Solid State Commun.* **61** (1987) 785.

5. K. SEDEEK and M. FADEL, *Thin Solid Films* **229** (1993) 223.
6. P. NAGELS, L. TICHY, H. TICHA and A. TRISKA, *J. Non-Cryst. Solids* **77**, **78** (1985) 1265.
7. N. TOHGE, Y. YONESAKI and T. MINAMI, *J. Appl. Phys.* **58** (1985) 4225.
8. S. R. ELLIOTT and A. T. STEEL, *Phys. Rev. Lett.* **57** (1986) 1316.
9. K. L. BAHATIA, D. P. GOSAIN, G. PARATHASARATHY and E. S. R. GOPAL, *J. Non-Cryst. Solids* **86** (1986) 65.
10. *Idem*, *Phys. Rev.* **B34** (1986) 8786.
11. J. C. PHILLIPS, *ibid.* **B36** (1987) 4265.
12. L. CERVINKA, J. BEREROVA and L. TICHY, *J. Non-Cryst. Solids* **192, 193** (1995) 45.
13. M. POLCIK, J. DRAHOKOUPIL, I. DRBOHLAV and L. TICHY, *ibid.* **192**, 193 (1995) 380.
14. E. MYLILINEAU, B. S. CHAO and D. PAPADIMITRIOU, *ibid.* **195** (1996) 279.
15. M. FADEL and K. SEDEEK, *Int. J. Chem.* **3** (1992) 245.
16. A. BECH, *J. Sci. Instrum.* **34** (1957) 186.
17. N. A. HEGAB, M. FADEL and K. SEDEEK, *Vacuum* **45** (1994) 459.
18. K. SEDEEK and M. FADEL, Unpublished work.
19. C. J. GLASSBRENNER and G. A. SLACK, *Phys. Rev.* **134** (1964) 1058.
20. A. R. REGEL, I. A. SMIRNOV and E. V. SHADRICHEV, *J. Non-Cryst. Solids* **8**–**10** (1972) 266.
21. S. H. LEE, H. K. HENISCH and W. D. BURGESS, *ibid.* **8**–**10** (1972) 422.
22. C. KITTLE, "Introduction to Solid State Physics", 6th edn (Wiley, New York, 1986) p. 116.
23. L. STOURAC, V. VASKO, I. SRB, C. MUSIL and F. STRABA, *Czech. J. Phys.* **B18** (1968) 1067.
24. K. N. AMIRKHANOV, Y. B. MAGOMEDOV, M. A. AIDAMIROV, L. G. AIO, K. O. A. ALIEVA and S. M. ISMAILOV, *Sov. J. Glass Phys. Chem.* (*USA*) **6** (1981) 219 (translated from *Fizika I. Khimia Stekla* **6** (1980) 312).
25. J. C. PHILLIPS, *J. Non-Cryst. Solids* **55** (1983) 179.
26. L. KOUDELKA, L. TICHY and M. PISARCIK, *J. Mater. Sci. Lett.* **11** (1992) 1060.
27. N. F. MOTT and E. A. DAVIS, "Electronic Processes In Non Crystalline Materials", 2nd edn (Clarendon Press, Oxford, 1979) p. 219.
28. V. K. BHATNAGAR, K. L. BAHATIA, D. P. GOSIN and V. K. JAIN, *J. Non-Cryst. Solids* **92** (1987) 302.
29. L. TICHY, H. TICHA, L. BENES and J. MLEK, *ibid.* **116** (1990) 206.
30. E. MARQUEZ, P. VILLARES and R. JIMENEZ-GARAY, *ibid.* **74** (1985) 195.
31. D. ADLER, "Disorder Materials: Science and Technology. Selected Papers" edited by S. R. Ovshinsky (Amorphous Institute Press, 1982) p. 220.
32. Y. ASAHARA and I. IZUMITANI, *Jpn. J. Appl. Phys.* **11** (1972) 109.
33. K. SHIMAKAWA, Y. INAGAKI and T. ARIZUMI, *ibid.* **12** (1973) 1043.
34. M. A. AFIFI, N. A. HEGAB, H. H. LABIB and M. FADEL, *Indian J. Pure Appl. Phys.* **30** (1992) 211.
35. J. I. PANKOVE, "Optical Processes in Semiconductors" (Dover, New York, 1975) p. 94.
36. M. H. COHEN, *J. Non-Cryst. Solids* **4** (1970) 391.
37. H. FRITZCHE, *ibid.* **6** (1971) 49.
38. K. SEDEEK, Doctorat es Sciènce, Marseille (1987).
39. R. SWANEPOEL, *J. Phys. E. Sci. Instrum.* **16** (1983) 1214.
40. D. R. PENN, *Phys. Rev.* **128** (1962) 2093.

Received 28 May 1997
and accepted 23 June 1998.